

Communication

**Rare Examples of Fe(IV) Alkyl-Imide Migratory Insertions:
Impact of Fe-C Covalency in (MeI₂)Fe(=NAd)R (R = Pe, 1-nor)**

Brian P. Jacobs, Peter T Wolczanski, Quan Jiang, Thomas R. Cundari, and Samantha N MacMillan

J. Am. Chem. Soc., Just Accepted Manuscript • DOI: 10.1021/jacs.7b06960 • Publication Date (Web): 10 Aug 2017

Downloaded from <http://pubs.acs.org> on August 10, 2017

Just Accepted

"Just Accepted" manuscripts have been peer-reviewed and accepted for publication. They are posted online prior to technical editing, formatting for publication and author proofing. The American Chemical Society provides "Just Accepted" as a free service to the research community to expedite the dissemination of scientific material as soon as possible after acceptance. "Just Accepted" manuscripts appear in full in PDF format accompanied by an HTML abstract. "Just Accepted" manuscripts have been fully peer reviewed, but should not be considered the official version of record. They are accessible to all readers and citable by the Digital Object Identifier (DOI®). "Just Accepted" is an optional service offered to authors. Therefore, the "Just Accepted" Web site may not include all articles that will be published in the journal. After a manuscript is technically edited and formatted, it will be removed from the "Just Accepted" Web site and published as an ASAP article. Note that technical editing may introduce minor changes to the manuscript text and/or graphics which could affect content, and all legal disclaimers and ethical guidelines that apply to the journal pertain. ACS cannot be held responsible for errors or consequences arising from the use of information contained in these "Just Accepted" manuscripts.



ACS Publications

Journal of the American Chemical Society is published by the American Chemical Society. 1155 Sixteenth Street N.W., Washington, DC 20036

Published by American Chemical Society. Copyright © American Chemical Society. However, no copyright claim is made to original U.S. Government works, or works produced by employees of any Commonwealth realm Crown government in the course of their duties.

1
2
3
4
5
6
7
8
9
10
11
12

Rare Examples of Fe(IV) Alkyl-Imide Migratory Insertions: Impact of Fe-C Covalency in $(\text{Me}_2\text{IPr})\text{Fe}(=\text{NAd})\text{R}_2$ ($\text{R} = ^{\text{neo}}\text{Pe}$, 1-nor)

Brian P. Jacobs,^a Peter T. Wolczanski*,^a Quan Jiang,^b Thomas R. Cundari*,^b and Samantha N. MacMillan^a

^aDepartment of Chemistry & Chemical Biology, Baker Laboratory, Cornell University, Ithaca, New York 14853

^bDepartment of Chemistry, CASCaM, University of North Texas, Denton, Texas, 76201

Supporting Information Placeholder

ABSTRACT: The iron(IV) imide complexes, $(\text{Me}_2\text{IPr})\text{R}_2\text{Fe}=\text{NAd}$ ($\text{R} = ^{\text{neo}}\text{Pe}$ (**3a**), 1-nor (**3b**)) undergo migratory insertion to iron(II) amides $(\text{Me}_2\text{IPr})\text{RFe}\{\text{NR}(\text{Ad})\}$ ($\text{R} = ^{\text{neo}}\text{Pe}$ (**4a**), 1-nor (**4b**))) without evidence of imidyl or free nitrene character. By increasing the field strength about iron, odd-electron reactivity was circumvented via increased covalency.

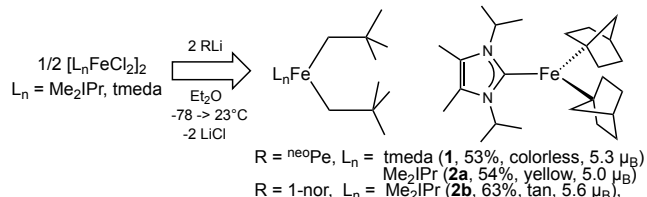
Recent investigations of iron imido complexes¹ feature species exhibiting imidyl (nitrogen radical, RN^\cdot) reactivity in the context of carbon-hydrogen bond activation²⁻⁷ to remarkably stable high oxidation state species.⁸⁻¹² The imidyl, "nitrene-insertion" reactivity, such as that described by Betley,² can be construed as a rebound process in which hydrogen atom transfer (HAT) is followed by coupling of carbon- and nitrogen-based radicals. Aziridinations^{2-7,13} often accompany or appear related to HAT initiated reactions, and can be considered as complementary, stepwise radical additions to olefins.

Classical imido (RN^2+) complexes are often unreactive, but in combination with electrophilic (d^0) early transition metal sites, can activate aliphatic CH bonds, including that of CH_4 , in a clear *concerted* fashion.^{14,15} Can iron complexes also exhibit such behavior? The covalency of related Fe(IV) imides must be extremely high in order to attenuate imidyl character, and strong field ligands such as alkyls and N-heterocyclic carbenes are attractive ancillary ligands.¹⁶ Herein are described formally Fe(IV) imido complexes that exhibit migratory insertion behavior best construed as concerted. The reactions are rare examples of $\text{L}_m\text{M}^n(=\text{X})\text{R} \rightarrow \text{L}_m\text{M}^{(n-2)}\text{-X-R}$ ($\text{X} = \text{O},^{17} \text{NR}'^{18-20}$) insertions that incur a formal oxidation state change, and portend the possibility of reactions such as olefin metathesis with first-row transition metal systems.

A variety of pseudo-tetrahedral $\text{L}_n\text{Fe}(^{\text{neo}}\text{Pe})_2$ complexes were targeted to avoid β -H-elimination paths, and synthesized via metathetical procedures²¹⁻²⁷ from corresponding halides. Upon treatment with various oxidants, including azides,²⁸ 2,2,5,5-tetramethylhexane was detected with few exceptions. Exposure of $(\text{tmeda})\text{Fe} (^{\text{neo}}\text{Pe})_2$ (1, $S = 2$, Scheme 1) to AdN_3 ($\text{Ad} = 1$ -adamantyl) afforded $\text{AdN}=\text{CH}^t\text{Bu}$, and no R-R coupling, suggestive of a nitrene insertion process.

$(^{\text{neo}}\text{Pe})_2$ (**1**, $S = 2$, Scheme 1) to AdN_3 ($\text{Ad} = 1$ -adamantyl) afforded $\text{AdN}=\text{CH}^t\text{Bu}$, and no R-R coupling, suggestive of a nitrene insertion process.

Scheme 1. Syntheses of L_nFeR_2 .



In order to generate a strong field, three-coordinate environment likely to induce imide formation, bulky Me_2IPr ²⁶⁻²⁹ was utilized as an ancillary ligand. 1-Norbornyl (nor) was another featured alkyl, as β -H-elimination is obviated by the formation of bridgehead olefins, and there is a history of 1-nor providing exceptionally strong fields,³⁰ as in $\text{Fe}(1\text{-nor})_4$.^{23,31,32}

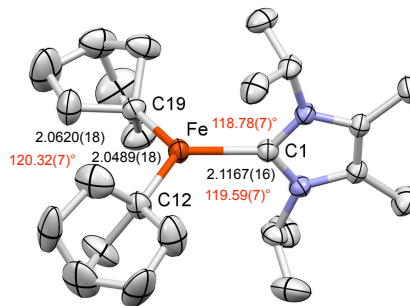


Fig. 1. Molecular view of $(\text{Me}_2\text{IPr})\text{Fe}(1\text{-nor})_2$ (**2b**); selected bond distances (black, Å) and angles (red) are given.

$(\text{Me}_2\text{IPr})\text{Fe}(^{\text{neo}}\text{Pe})_2$ (**2a**) and $(\text{Me}_2\text{IPr})\text{Fe}$ (nor)₂ (**2b**) were prepared from metathesis of $[(\text{Me}_2\text{IPr})\text{FeCl}_2]_2$ with $^{\text{neo}}\text{PeLi}$ and (1-nor)Li, respectively (Scheme 1) and possess μ_{eff} values of 5.0 (**2a**) and 5.6 μ_{B} (**2b**),³³ indicative of $S = 2$ centers. A molecular view of **2b** is given in Fig. 1, along with core interatomic distances and angles. Three-coordinate **2b** is nearly trigonal despite the steric bulk of the tertiary 1-norbornyl substituents. A similar

geometry is observed for $(\text{Me}_2\text{IPr})\text{Fe}(\text{neoPe})_2$ (**2a**, X-ray) but severe twinning problems hampered refinement.

Exposure of $(\text{Me}_2\text{IPr})\text{Fe}(\text{neoPe})_2$ (**2a**) to AdN_3 afforded a persistent dark green solution at -78°C that slowly became yellow at 23°C . ^1H NMR spectroscopy, protic quenching studies that yielded $\text{AdNH}(\text{neoPe})$, and X-ray crystallography revealed the migratory insertion product, $(\text{Me}_2\text{IPr})\text{Fe}\{\text{N}(\text{Ad})\text{neoPe}\}(\text{neoPe})$ (**4a**, 65%), as shown in Scheme 2. Its μ_{eff} of $5.1 \mu_B^{33}$ was consistent with an $S = 2$ ferrous center.

Scheme 2. $(\text{Me}_2\text{IPr})\text{Fe}(\text{=NAdR}_2)$ to $(\text{Me}_2\text{IPr})\text{Fe}\{-\text{N}(\text{Ad})-\text{R}\}\text{R}$ ($\text{R} = \text{neoPe}$, **3a**→**4a**; 1-nor, **3b**→**4b**).

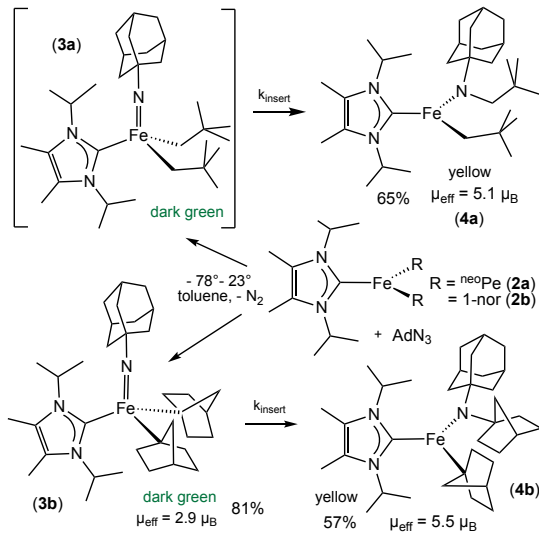


Fig. 2 illustrates a molecular view of $(\text{Me}_2\text{IPr})\text{Fe}\{\text{N}(\text{Ad})\text{neoPe}\}(\text{neoPe})$ (**4a**), which exhibits a slightly distorted trigonal structure with the Me_2IPr ligand again vertical to the trigonal plane. Core bond distances are normal for a low coordinate high spin ferrous center, and the $d(\text{FeC})$ for the neopentyl ligand is $\sim 0.07 \text{ \AA}$ shorter than the corresponding NHC interaction.

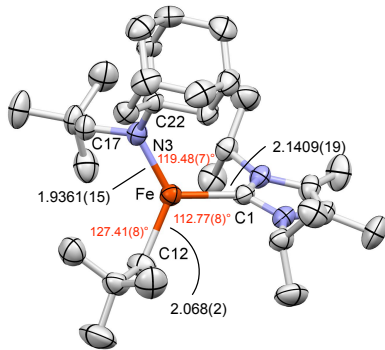


Fig. 2. View of $(\text{Me}_2\text{IPr})\text{Fe}\{\text{N}(\text{Ad})\text{neoPe}\}(\text{neoPe})$ (**4a**); selected bond distances (black, Å) and angles (red) are given.

Failure to isolate dark green **3a** prompted a switch to $(\text{Me}_2\text{IPr})\text{Fe}(1\text{-nor})_2$ (**2b**).^{23,31,32} Treatment of **2b** with AdN_3 under identical conditions permitted isolation of

dark green $(\text{Me}_2\text{IPr})\text{Fe}(\text{=NAd})(1\text{-nor})_2$ (**3b**, 81%), and its μ_{eff} of $2.9 \mu_B^{33}$ revealed an intermediate spin ($S = 1$) system. Imide **3b** was thermally converted to the yellow insertion product, $(\text{Me}_2\text{IPr})\text{Fe}\{\text{N}(\text{Ad})(1\text{-nor})\}(1\text{-nor})$ (**4b**, 57%, $S = 2$, $\mu_{\text{eff}} = 5.5 \mu_B$), and protic quenching of **4b** provided $\text{AdNH}(1\text{-nor})$. Spectroscopic characteristics relating **3b** to **3a** suggested the latter to be the thermally unstable imide, $(\text{Me}_2\text{IPr})\text{Fe}(\text{=NAd})(\text{neoPe})_2$ (**3a**).

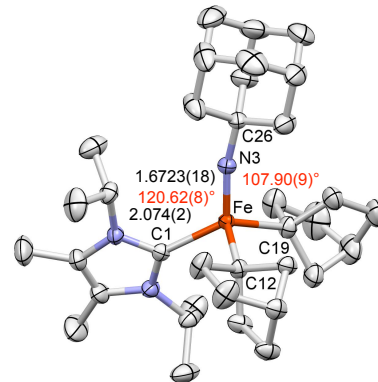


Fig. 3. Molecular view of $(\text{Me}_2\text{IPr})\text{Fe}(\text{=NAd})(1\text{-nor})_2$ (**3b**). Selected bond distances (black, Å) and angles (red, °): Fe-C12, 2.005(2); Fe-C19, 2.024(2); N3-C26, 1.437(3); N3-Fe-C12, 105.09(9); C12-Fe-C19, 103.77(9); C1-Fe-C12, 96.98(8); C1-Fe-C19, 119.23(9); Fe-N3-C26, 168.04(15).

Fig. 3 shows the distorted tetrahedral structure of $(\text{Me}_2\text{IPr})\text{Fe}(\text{=NAd})(1\text{-nor})_2$ (**3b**), highlighting its short ($1.6723(18) \text{ \AA}$), nearly linear ($168.04(15)^\circ$) iron imide linkage. The distorted core appears to reflect steric interactions, as the adamantly unit is tipped away from the iPr group on the Me_2IPr , although the 1-nor ligands span a C12-Fe-C19 angle of only $103.77(9)^\circ$. Favorable dispersion forces, specifically in Fe(IV) complexes, appear to play a role in stabilization of hindered systems.^{23,34}

Calculations (B3PW91-GD3/6-31+G(d)) of $(\text{Me}_2\text{IPr})\text{Fe}(\text{=NAd})(1\text{-nor})_2$ (**3b**) confirm an $S = 1$ ground state. There is an impressive admixture of 1-nor and Me_2IPr character to the $\text{Fe}(\text{d}\pi)\text{-N}(\text{p}\pi)$ frontier orbitals of **3b** (6 α - and 4 β -orbitals span 0.10 eV), such that correlating spins and defining a ligand field (d^0) are subjective. The significant amounts of iron and carbon character are consistent with strong covalent interactions that belie the formal Fe(IV) oxidation state.³⁵

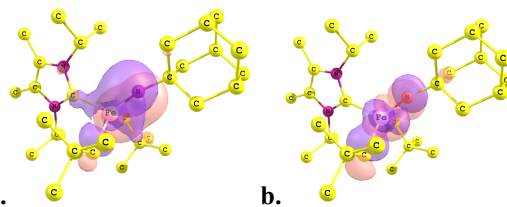


Fig. 4. CAS(14,14) natural orbitals of **3a** (contour value = 0.03): **a.** $\text{FeC}(\sigma)$ (neoPe) with $\text{FeN}(\pi)$; **b.** $\text{FeN}(\pi^*)$.

1
2
3
4
5
6
7
8
9
10
11
12
13
14
15
16
17
18
19
20
21
22
23
24
25
26
27
28
29
30
31
32
33
34
35
36
37
38
39
40
41
42
43
44
45
46
47
48
49
50
51
52
53
54
55
56
57
58
59
60

MCSHF calculations were conducted at the DFT-optimized geometry of **3a**. Within the CAS(14,14) active space, MCSHF natural orbitals show significant delocalization, particularly four nearly doubly occupied (natural orbital population $\sim 1.9 \text{ e}^-$) orbitals with mixed FeC(σ), (${}^{\text{neo}}\text{Pe}$), and FeN(π) character (Fig. 4a.). Next highest in energy are two singly occupied orbitals that are primarily Fe(3d) in character, followed by two natural orbitals (occupation $\sim 0.1 \text{ e}^-$) that are FeN(π^*) (Fig. 4b.). The total Mulliken population of Fe among the 14 active space natural orbitals is 6.9 e^- ,³⁵ implying significant covalency and charge delocalization among all iron-ligand bonds.

Table 1. Migratory insertion rates of $(\text{Me}_2\text{IPr})\text{Fe}(=\text{N}-\text{Ad})\text{R}_2$ ($\text{R} = {}^{\text{neo}}\text{Pe}$, **3a**; 1-nor, **3b**) to $(\text{Me}_2\text{IPr})\text{Fe}\{\text{N}(\text{R})\text{Ad}\}\text{R}_2$ ($\text{R} = {}^{\text{neo}}\text{Pe}$, **4a**; 1-nor, **4b**).^a

rxn	T($\pm 1.0^\circ\text{C}$)	k (s^{-1})	ΔG^\ddagger
3a \rightarrow 4a ^b	-10.0	$4.85(8)\times 10^{-5}$	20.5(8)
3a \rightarrow 4a ^b	1.0	$2.84(29)\times 10^{-4}$	20.4(8)
3a \rightarrow 4a ^b	10.0	$1.17(8)\times 10^{-3}$	20.3(8)
3a \rightarrow 4a ^b	21.0	$4.78(30)\times 10^{-3}$	20.3(8)
3a \rightarrow 4a ^b	30.0	$1.37(8)\times 10^{-2}$	20.3(8)
3b \rightarrow 4b ^c	23.0	$4.85(8)\times 10^{-5}$	24.0(6)
3b \rightarrow 4b ^c	40.0	$2.84(29)\times 10^{-4}$	24.0(6)
3b \rightarrow 4b ^c	50.0	$1.17(8)\times 10^{-3}$	24.0(6)
3b \rightarrow 4b ^c	60.0	$4.78(30)\times 10^{-3}$	24.0(6)
3b \rightarrow 4b ^c	71.0	$1.37(8)\times 10^{-2}$	24.0(6)

^aToluene-*d*₈. ^b[**3a**] = 0.057 M; $\Delta H^\ddagger = 22.3(8)$, $\Delta S^\ddagger = 6.5(1)$ eu. ^c[**3b**] = 0.047 M; $\Delta H^\ddagger = 24.4(6)$, $\Delta S^\ddagger = 1.3(1)$ eu.

$(\text{Me}_2\text{IPr})\text{Fe}(=\text{NAd})({}^{\text{neo}}\text{Pe})_2$ (**3a**) could not be isolated, but it persisted in solution for a time sufficient to evaluate the insertion kinetics. $(\text{Me}_2\text{IPr})\text{Fe}(=\text{NAd})(1\text{-nor})_2$ (**3b**) could be similarly analyzed, and the results are listed in Table 1. The migratory insertion of **3a** to $(\text{Me}_2\text{IPr})\text{Fe}\{\text{N}(\text{Ad})({}^{\text{neo}}\text{Pe})\}({}^{\text{neo}}\text{Pe})$ (**4a**, $\Delta G^\ddagger(25^\circ) = 20.4(8)$ kcal/mol) is ~ 3.6 kcal/mol more favorable than the conversion of **3b** to $(\text{Me}_2\text{IPr})\text{Fe}\{\text{N}(\text{Ad})(1\text{-nor})\}(1\text{-nor})$ (**4b**, $\Delta G^\ddagger(25^\circ) = 24.0(6)$ kcal/mol). Enthalpy ($\Delta\Delta H^\ddagger \sim 2.1$) and entropy ($\Delta\Delta S^\ddagger \sim 5.2$ eu) differences impart roughly the same changes in $\Delta\Delta G^\ddagger$.

Only additions of AdN_3 to **2e** and **3e** enabled spectroscopic observation of the Fe(IV) imide, but exposure of R'N₃ to various dialkyls ($\text{Me}_2\text{IPr})\text{FeR}_2$ ($\text{R} = {}^{\text{neo}}\text{Pe}$, **2a**; 1-nor, **2b**; mesityl (Mes)) enabled rough relative amide formation rates to be obtained: $\text{R} = \text{Mes} \sim {}^{\text{neo}}\text{Pe} > 1\text{-nor}; \text{R}' = \text{Ph} > \text{SiMe}_3 > \text{Ad}$. In the presence of cyclohexene, 1,4-cyclohexadiene, or Et_3SiH , the **3b** to **4b** conversion was unaffected, and products from nitrene trapping were not observed. Slow alkyl exchanges are rampant, as **2a** and **2b** equilibrate with $(\text{Me}_2\text{IPr})\text{Fe}({}^{\text{neo}}\text{Pe})(1\text{-nor})$ (**2ab**), **2b** and **4a** with $(\text{Me}_2\text{IPr})\text{Fe}\{\text{N}(\text{Ad})({}^{\text{neo}}\text{Pe})\}(1\text{-nor})$ and **2ab**, and **4b** and **2a** with $(\text{Me}_2\text{IPr})\text{Fe}\{\text{N}(\text{Ad})(1\text{-nor})\}({}^{\text{neo}}\text{Pe})$ and **2ab** in near statistical mixtures. Despite these complications, transiently generated **3a** provided

4a when an equiv of **2b** was present, indicative of an intramolecular migratory insertion.

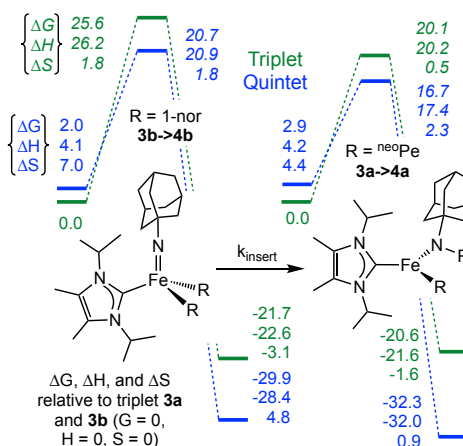


Fig. 5. Triplet (green) and quintet (blue) surfaces for the **3b** \rightarrow **4b** and **3a** \rightarrow **4a** migratory insertions; ΔG and ΔH are in kcal/mol and ΔS is in eu; transition states are in *italics*.

Calculations were conducted to gain insight into the reaction coordinate for insertion. Following the success of Power *et al.*,³⁴ B3PW91-GD3/G-31+G(d) simulations were applied to the migratory insertions. Fig. 5 shows that the computations reproduce the lower barrier for **3a** \rightarrow **4a** ($\text{R} = {}^{\text{neo}}\text{Pe}$) over **3b** \rightarrow **4b** ($\text{R} = 1\text{-nor}$): $\Delta\Delta G^\ddagger(298\text{K}) = 3.6$ kcal/mol, $\Delta\Delta G^\ddagger(\text{calc}) = 4.0$ kcal/mol. The requisite spin-flip from the triplet imide surface to the quintet amide surface occurs prior to the transition state for insertion in both instances.

The favorable $\Delta\Delta G^\ddagger$ of -2.4 kcal/mol for **4a** formation relative to **4b** is mostly enthalpic in origin, and the $\Delta\Delta H^\ddagger$ of -3.5 kcal/mol favoring the ${}^{\text{neo}}\text{Pe}$ -based conversion closely corresponds to the accompanying $\Delta\Delta H^\ddagger$ of -3.6 kcal/mol. Subtle entropic factors also favor the less rigid ${}^{\text{neo}}\text{Pe}$ system as the change from 4- to 3-coordinate frees up conformational space.

Table 2. Calculated^a BDEs and BDDEs for ground states (GSs) of $(\text{Me}_2\text{IPr})\text{YFe-R}$ ($[\text{Fe}] = (\text{Me}_2\text{IPr})\text{Fe}$).^b

iron alkyl cmpnd	BDE	BDDE
$[\text{Fe}]({}^{\text{neo}}\text{Pe})_2$ (2a)	51.1	35.5
$[\text{Fe}](1\text{-nor})_2$ (2b)	57.0	42.2
$(\text{AdN}=)[\text{Fe}]({}^{\text{neo}}\text{Pe})_2$ (3a)	36.5 ^c	18.1 ^c
	32.3 ^d	15.2 ^d
$(\text{AdN}=)[\text{Fe}](1\text{-nor})_2$ (3b)	43.5	26.0
	39.5	24.0
$\{\text{N}(\text{Ad})({}^{\text{neo}}\text{Pe})\}[\text{Fe}]({}^{\text{neo}}\text{Pe})$ (4a)	53.8	36.2
$\{\text{N}(\text{Ad})(1\text{-nor})\}[\text{Fe}](1\text{-nor})$ (4b)	55.5	41.2

^a B3PW91-GD3/G-31+G(d). ^b [Fe] = $(\text{Me}_2\text{IPr})\text{Fe}$. ^c Triplet GS. ^d Quintet excited state (ES).

Why does the neopentyl system manifest a greater insertion rate and more favorable thermodynamics? Insight was obtained via BDE and BDDE calculations of

the various D(FeR). The favorable thermodynamics for **3a**→**4a** vs. **3b**→**4b** tracks with iron-alkyl bond energy differences as the iron(IV) imide converts to the iron(II)amide (Table 2). The iron-alkyl bonds exhibit greater changes ($\Delta\Delta H = -17.3$ vs. -12.0 kcal/mol; $\Delta\Delta G = -18.1$ vs. -15.2 kcal/mol) in the ^{neo}Pe system over the 1-norbornyl complexes, despite the latter having larger magnitudes due to the greater s-character of the constrained bridgehead position.

In summary, an increase in covalency enables formally Fe(IV) dialkyl-imides to manifest a rare migratory insertion reaction intrinsic to strong field systems. The chemistry provides hope that $2e^-$ reactivity, such as olefin metathesis, may be possible in formally high oxidation state first-row transition metal systems.

ASSOCIATED CONTENT

Supporting Information. Experimental details on procedures and reactions; X-ray crystallographic information pertaining to **1**, **2a**, **2b**, **3b**, and **4a**.

AUTHOR INFORMATION

Corresponding Authors

e-mail: ptw2@cornell.edu; t@unt.edu

Notes

The synthesis and structure of (tmada)Fe(^{neo}Pe)₂ (**1**) have also been done by E. B. Hulley *et al.* (Univ. Wyoming).

ACKNOWLEDGMENT

We thank the NSF (PTW: CHE-1402149; CHE-1664580; TRC: CHE-1531468 (CASCaM)), and the DOE (TRC: DE-FG02-03ER15387) for financial support.

REFERENCES

- (1) (a) Saouma, C. T.; Peters, J. C. *Coord. Chem. Rev.* **2011**, *255*, 920-937. (b) Mehn, M. P.; Peters, J. C. *J. Inorg. Biochem.* **2006**, *100*, 634-643.
- (2) (a) Hennessy, E. T.; Liu, R. Y.; Iovan, D. A.; Duncan, R. A.; Betley, T. A. *Chem. Sci.* **2014**, *5*, 1526-1532. (b) Hennessy, E. T.; Betley, T. A. *Science* **2013**, *340*, 591-595. (c) King, E. R.; Hennessy, E. T.; Betley, T. A. *J. Am. Chem. Soc.* **2011**, *133*, 4917-4923. (d) Iovan, D. A.; Betley, T. A. *J. Am. Chem. Soc.* **2016**, *138*, 1983-1993.
- (3) (a) Chow, T. W.-S.; Chen, G.-Q.; Liu, Y. G.; Zhou, C.-Y.; Che, C.-M. *Pure. Appl. Chem.* **2012**, *84*, 1685-1704. (b) Liu, Y. G.; Guan, X. G.; Wong, E. L. M.; Liu, P.; Huang, J. S.; Che, C.-M. *J. Am. Chem. Soc.* **2013**, *135*, 7194-7204.
- (4) Jensen, M. P.; Mehn, M. P.; Que, L. *Angew. Chem. Int. Ed.* **2003**, *42*, 4357-4360.
- (5) Paradine, S. M.; White, M. C. *J. Am. Chem. Soc.* **2012**, *134*, 2036-2039.
- (6) Cowley, R. E.; Golder, M. R.; Eckert, N. A.; Al-Afyouni, M. H.; Holland, P. L. *Organometallics* **2013**, *32*, 5289-5298. (b) Cowley, R. E.; Holland, P. L. *Inorg. Chem.* **2012**, *51*, 8352-8361.
- (7) Gouré, E.; Avenier, F.; Dubourdeaux, P.; Séneque, O.; Albrieux, F.; Lebrun, C.; Clémancey, M.; Maldivi, P.; Latour, J.-M. *Angew. Chem. Int. Ed.* **2014**, *53*, 1580-1584.
- (8) (a) Brown, S. D.; Betley, T. A.; Peters, J. C. *J. Am. Chem. Soc.* **2003**, *125*, 322-323. (b) Brown, S. D.; Peters, J. C. *J. Am. Chem. Soc.* **2004**, *126*, 4538-4539. (c) Moret, M.-E.; Peters, J. C. *Angew. Chem. Int. Ed.* **2011**, *50*, 2063-2067. (d) Thomas, C. M.; Mankad, N. P.; Peters, J. C. *J. Am. Chem. Soc.* **2006**, *128*, 4956-4957.
- (9) Mehn, M. P.; Brown, S. D.; Jenkins, D. M.; Peters, J. C.; Que Jr., L. *Inorg. Chem.* **2006**, *45*, 7417-7427.
- (10) Ni, C.; Fettinger, J. C.; Long, G. J.; Brynda, M.; Power, P. P. *Chem. Commun.* **2008**, 6045-6047.
- (11) (a) Wang, L.; Hu, L.; Zhang, H.; Chen, H.; Deng, L. *J. Am. Chem. Soc.* **2015**, *137*, 14196-14207. (b) Zhang, H. Z.; Ouyang, Z. W.; Liu, Y. S.; Zhang, Q.; Wang, L.; Deng, L. *Angew. Chem. Int. Ed.* **2014**, *53*, 8432-8436.
- (12) Nieto, I.; Ding, F.; Bontchev, R. P.; Wang, H.; Smith, J. M. *J. Am. Chem. Soc.* **2008**, *130*, 2716-2717.
- (13) Heins, S. P.; Morris, W. D.; Wolczanski, P. T.; Lobkovsky, E. B. *Angew. Chem. Int. Ed.* **2015**, *54*, 14407-14411.
- (14) (a) Bennett, J. L.; Wolczanski, P. T. *J. Am. Chem. Soc.* **1997**, *119*, 10696-10719. (b) Cummins, C. C.; Baxter, S. M.; Wolczanski, P. T. *J. Amer. Chem. Soc.* **1988**, *110*, 8731-8733.
- (15) (a) Hoyt, H. M.; Michael, F. E.; Bergman, R. G. *J. Am. Chem. Soc.* **2004**, *126*, 1018-1019. (b) Walsh, P. J.; Hollander, F. J.; Bergman, R. G. *J. Amer. Chem. Soc.* **1988**, *110*, 8729-8731.
- (16) (a) Lindley, B. M.; Swidan, A.; Lobkovsky, E. B.; Wolczanski, P. T.; Adelhardt, M.; Sutter, J.; Meyer, K. *Chem. Sci.* **2015**, *6*, 4730-4736. (b) Lindley, B. M.; Jacobs, B. P.; MacMillan, S. N.; Wolczanski, P. T. *Chem. Commun.* **2016**, *52*, 3891-3894.
- (17) (a) Brown, S. N.; Mayer, J. M. *J. Am. Chem. Soc.* **1996**, *118*, 12119-12133. (b) Brown, S. N.; Mayer, J. M. *J. Am. Chem. Soc.* **1994**, *116*, 2219-2220.
- (18) Hu, X.; Meyer, K. *J. Am. Chem. Soc.* **2004**, *126*, 16322-16323.
- (19) (a) Matsunaga, P. T.; Hess, C. R.; Hillhouse, G. L. *J. Am. Chem. Soc.* **1994**, *116*, 3665-3666. (b) Koo, K.; Hillhouse, G. L. *Organometallics* **1996**, *15*, 2669-2271.
- (20) Cenini, S.; Gallo, E.; Caselli, A.; Ragaini, F.; Fantauzzi, S.; Piangolini, C. *Coord. Chem. Rev.* **2006**, *250*, 1234-1253.
- (21) Fürstner, A.; Martin, R.; Krause, H.; Seidel, G.; Goddard, R.; Lehmann, C. W. *J. Am. Chem. Soc.* **2008**, *130*, 8773-8787.
- (22) (a) Al-Afyouni, M. H.; Fillman, K. L.; Brennessel, W. W.; Neidig, M. L. *J. Am. Chem. Soc.* **2014**, *136*, 15457-15460. (b) Muñoz III, S. B.; Daifuku, S. L.; Brennessel, W. W.; Neidig, M. L. *J. Am. Chem. Soc.* **2016**, *138*, 7492-7495.
- (23) Casitas, A.; Rees, J. A.; Goddard, R.; Bill, E.; DeBeer, S.; Fürstner, A. *Angew. Chem. Int. Ed.* **2017**, *56*, 0000.
- (24) (a) Fernández, I.; Trovitch, R. J.; Lobkovsky, E.; Chirik, P. J. *Organometallics* **2008**, *27*, 109-118. (b) Cámpora, J.; Naz, A. M.; Palma, P.; Álvarez, E.; Reyes, M. L. *Organometallics* **2005**, *24*, 4878-4881.
- (25) (a) Karsch, H. H. *Chem. Ber.* **1977**, *110*, 2699-2711. (b) Hermes, A. R.; Girolami, G. S. *Organometallics* **1987**, *6*, 763-768.
- (26) Xiang, L.; Xiao, J.; Deng, L. *Organometallics* **2011**, *30*, 2018-2025.
- (27) Danopoulos, A. A.; Braunstein, P.; Wesolek, M.; Monakhov, K. Y.; Rabu, P.; Robert, V. *Organometallics* **2012**, *31*, 4102-4105.
- (28) (a) Katsuki, T. *Chem. Lett.* **2005**, *34*, 1304-1309. (b) Huang, X. Y.; Bergsten, T. M.; Groves, J. T. *J. Am. Chem. Soc.* **2015**, *137*, 5300-5303.
- (29) Ryan, S. J.; Schimler, S. D.; Bland, D. C.; Sanford, M. S. *Org. Lett.* **2015**, *17*, 1866-1869.
- (30) Byrne, E. K.; Theopold, K. H. *J. Am. Chem. Soc.* **1989**, *111*, 3887-3896.
- (31) Bower, B. K.; Tennent, H. G. *J. Am. Chem. Soc.* **1972**, *94*, 2512-2514.
- (32) Lewis, R. A.; Smiles, B. E.; Darmon, J. M.; Stieber, S. C. E.; Wu, G.; Hayton, T. W. *Inorg. Chem.* **2013**, *52*, 8218-8227.
- (33) (a) Evans, D. F. *J. Chem. Soc.* **1959**, 2003-2005. (b) Schubert, E. M. *J. Chem. Ed.* **1992**, *69*, 62.
- (34) Liptrot, D. J.; Guo, J. D.; Nagase, S.; Power, P. P. *Angew. Chem. Int. Ed.* **2016**, *55*, 14766-14769.
- (35) Wolczanski, P. T. *Organometallics* **2017**, *36*, 622-631.

1 Table of Contents Graphic
2
3
4
5
6
7
8
9
10
11
12